Revista Brasileira de Farmacognosia 25 (2015) 690–697

Revista Brasileira de Farmacognosia
BRAZILIAN JOURNAL OF PHARMACOGNOSY
www.sbfgnosia.org.br/revista

Original article

Combined structure- and ligand-based virtual screening to evaluate caulerpin analogs with potential inhibitory activity against monoamine oxidase B

Vitor Prates Lorenzo[a,b], José Maria Barbosa Filho[a], Luciana Scotti[a], Marcus Tullius Scotti[a,*]

[a] Programa de Pós-graduação em Produtos Naturais e Sintéticos Bioativos, Universidade Federal da Paraíba, João Pessoa, PB, Brazil
[b] Instituto Federal do Sertão Pernambucano, Petrolina, PE, Brazil

ARTICLE INFO

Article history:
Received 30 April 2015
Accepted 9 August 2015
Available online 19 September 2015

Keywords:
Alzheimer's disease
Caulerpin
Molecular docking
Monoamine oxidase B
Virtual screening

ABSTRACT

Natural marine products can help increase the quality of life in patients with neurological diseases. A large number of marine products act against Alzheimer's disease through varying pathways. According to structure- and ligand-based analyses, caulerpin, an alkaloid primarily isolated from the genus *Caulerpa*, possesses activity against monoamine oxidase B. To predict the activity of caulerpin, we employed Volsurf descriptors and the machine learning Random Forest algorithm in parallel with a structure-based methodology that included molecular docking. Using caulerpin as a lead compound, a database containing 108 analogs was evaluated, and nine were selected as active. The structures selected as active exhibited polar and non-polar substitutions on the caulerpin skeleton, which were relevant for their activity. Dragon consensus drug-like scoring was applied to identify the active analogs that might serve as good drug candidates, and the entire group presented satisfactory performance. These results indicate the possibility of using these analogs as potential leads against Alzheimer's disease.

Introduction

Alzheimer's disease (AD) has emerged as the most prevalent type of late-life disorder in humans, afflicting 45% of people over 85 years old (Liu et al., 2013). This burden is increasing as the elderly population continues to grow. In general, AD is associated with neuronal loss, synaptic dysfunction and functional abnormalities of mitochondrial structures (LaFerla and Oddo, 2005). In the literature, different methods of controlling AD have been reported, which offer alternative mechanisms of action (Tian et al., 2014; Riediger et al., 2009). In an attempt to improve the quality of life for AD patients, numerous studies are being conducted to develop more efficient drugs.

The marine environment covers 70% of the earth's surface and provides a fascinating variety of biodiversity that exceeds that of the terrestrial environment. The biodiversity of the marine environment and its associated chemical diversity constitute a practically unlimited resource of new active substances that may potentially be developed into novel bioactive products (Souza et al., 2009a,b). The exploration of this biodiversity to identify new chemical compounds has only just begun. Marine organisms synthesize a plethora of small molecules with fascinating chemical structures and potent biological properties. The variety of marine organisms that have been discovered to date offers a dramatic potential pool of resources for drug discovery, and many new discoveries remain to be made (Bidon-Chanal et al., 2013; Schumacher et al., 2011; Gerwick and Moore, 2012).

Natural marine products play an important role in increasing the quality of life for patients with neurological diseases. These products include fatty acids (such as n-3 fatty acid, which delays the onset of AD), terpenes, alkaloids and varying other secondary metabolites, all of which act through different pathways (Choi et al., 2007; Gul and Hamann, 2005).

Several phlorotannins, such as eckstolonol [639514-05-9] (**1**), eckol [99798-74-7] (**2**) and phlorofucofuroeckol-A [128129-56-6]

* Corresponding author.
E-mail: mtscotti@ccae.ufpb.br (M.T. Scotti).

http://dx.doi.org/10.1016/j.bjp.2015.08.005
0102-695X/

(**3**), may represent useful nutraceuticals for the prevention of AD due to their inhibitory activities against acetylcholinesterase (AChE) and butylcholinesterase (BChE), which have been demonstrated *in vitro* (Thomas and Kim, 2011; Yoon et al., 2009). Hexane extracts of *Tetraselmis chuii*, *Chlorella minutissima* and *Rhodomonas salina* also exhibited cholinesterase inhibitory activity toward AChE (Custódio et al., 2012). Additional kinase inhibitors that are useful for the treatment of AD include steroidal alkaloid 4-acetoxy-plakinamine B [1003045-50-8] (**4**) (Langjae et al., 2007), sargaquinoic acid [70363-87-0] (**5**) and sargachromenol [70363-89-2]; the latter two are meroditerpenes (**6**) (Choi et al., 2007). Sargaquinoic acid was found to potently inhibit BChE, a novel target for the treatment of AD, with potency comparable to or greater than the anticholinesterases that are in current clinical use (Mayer et al., 2011). Potential AChE inhibitors have been discovered in extracts from *Latrunculia lendenfeldi* and *Latrunculia bocagei* sponges (Turk et al., 2013).

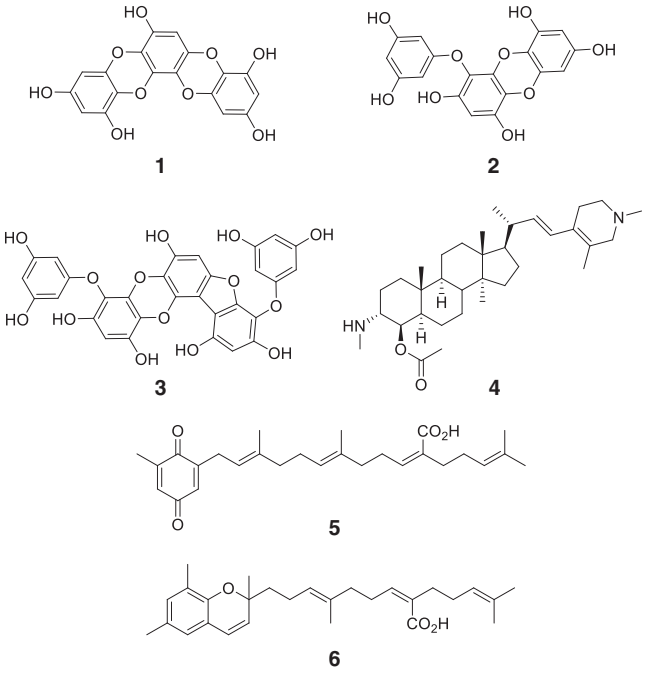

Additional studies have reported discoveries of novel glycogen synthase kinase 3β (GSK-3β) inhibitors in natural marine products (Jin et al., 2006). Examples of these active marine-derived compounds include palinurim [71947-64-3] (**7**) (Bidon-Chanal et al., 2013), lamellarin E [115982-19-9] (**8**) (Baunbaek et al., 2008), hymenialdisine [82005-12-7] (**9**) (Meijer et al., 2000), meridianine E [213473-03-1] (**10**) (Radwan and El-Sherbiny, 2007), manzamine A [104196-68-1] (**11**) (Hamann et al., 2007) and 6-Bromoindirubin [200273-66-1] (**12**) (Meijer et al., 2003). Palinurin, a furanosesquiterpene, inhibits GSK-3β activity through a novel mechanism of action (Bidon-Chanal et al., 2013). Debdab and collaborators have also reported the kinase inhibitory activities of derivatives of the marine alkaloid leucettamine B [147395-96-8] (**13**) (Debdab et al., 2010).

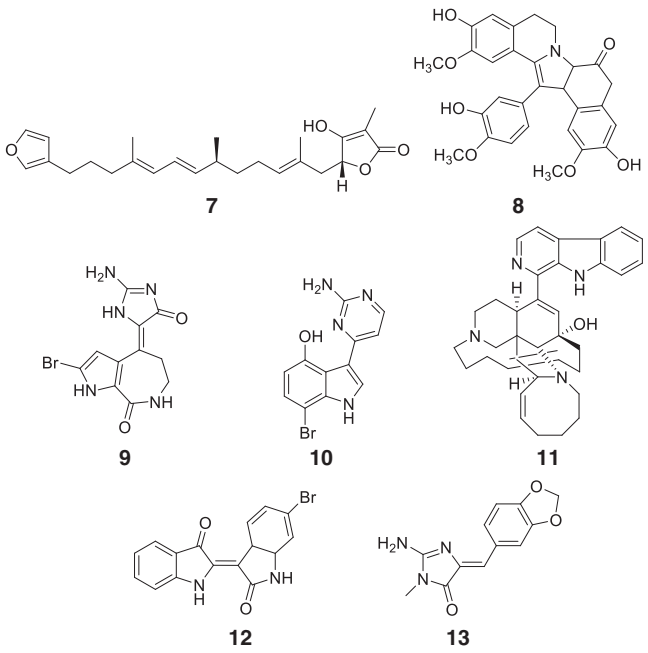

Tumescenamide A [1335094-05-7] (**14**) induces reporter gene expression under the control of the insulin-degrading enzyme (IDE) promoter, which suggests that it may have promise as a potential treatment for AD (Motohashi et al., 2010). The 3,5-dibromo-4-methoxyphenyl-pyruvic acid [1356930-31-8] (**15**), isolated from sponge Callyspongia sp., is able to modulate apolipoprotein E (ApoE) (Tian et al., 2014). Dragmacidin D [142979-34-8] (**16**) inhibits neural nitric oxide synthase, which may prove to be an option for the treatment of Huntington's, Parkinson's and Alzheimer's diseases (Yang et al., 2002).

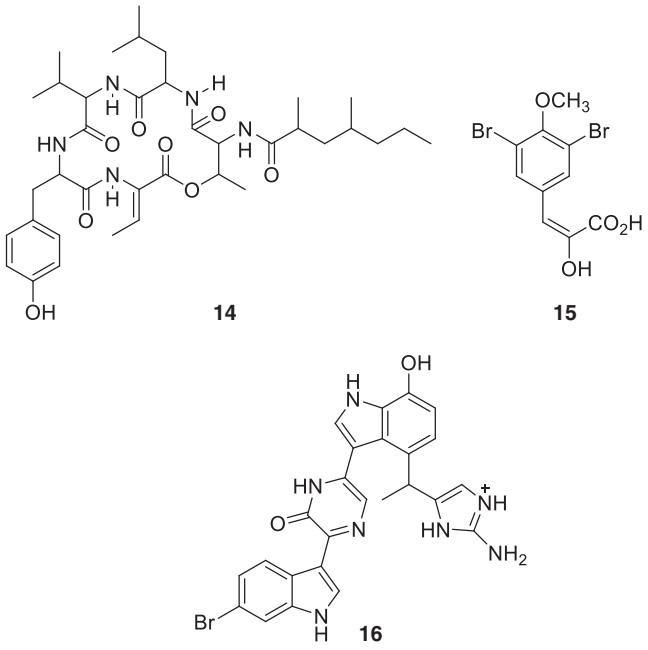

Monoamine oxidase (MAO) is a FAD-containing enzyme that catalyzes the oxidative deamination of a variety of biogenic and xenobiotic amines including monoamine neurotransmitters such as serotonin, noradrenaline and dopamine (Binda et al., 2011; Bolea et al., 2013). MAO plays an important role in the metabolism of several neurotransmitters and could therefore be useful in the treatment of a number of psychiatric and neurological diseases.

MAO activity helps to ensure that neuron firing rates throughout the body remain within homeostatic limits. MAO-B inhibitors, such as selegiline (R-(−)-deprenyl) [14611-52-0] (**17**) and rasagiline [161735-79-1] (**18**), are useful compounds for the symptomatic treatment of Parkinson's and Alzheimer's diseases (Zhu et al., 2008; Choi and Choi, 2015), as they increase concentrations of synaptic dopamine by blocking its degradation (Fernandez and Chen, 2007). Another MAO-B inhibitor, safinamide [133865-89-1] (**19**), is currently undergoing phase III clinical trials as an adjuvant in combination with a dopamine agonist or levodopa (Schapina, 2011). MAO-B inhibitors have also been extensively studied for their possible neuroprotective or disease-modifying actions, and there is an abundant amount of evidence that MAO-B inhibitors have some neuroprotective properties (Patil et al., 2013).

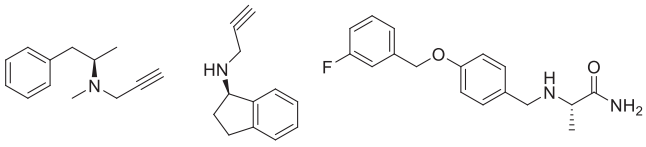

17 **18** **19**

Caulerpin [26612-48-6] (**20**, CLP 001) is a bisindole alkaloid that is primarily isolated from green algae of the genus *Caulerpa* (Souza et al., 2009a,b); it has an extra eight-member ring between the two indole rings, which are incorporated directly with the carbonyl group. Our research group has reported that caulerpin has a non-selective spasmolytic effect and that this effect is due in part to the inhibition of Ca^{2+} influx through voltage-gated calcium channels (Ca_v) (Cavalcante-Silva et al., 2013) and noticed for the first time that caulerpin has showed a considerable antinociceptive and anti-inflammatory activities (Souza et al., 2009a,b).

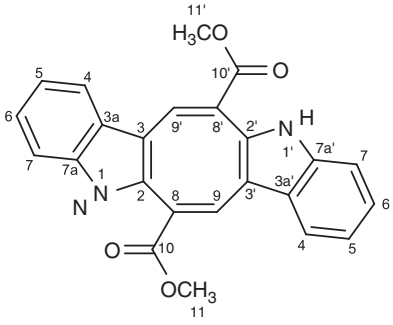

20
CLP 001

Computer-aided drug design (CADD) has become an indispensable tool to the pharmaceutical industry and academia over the last decade (Lill and Danielson, 2011) and has been employed during various stages of the drug-design process. Initially, this method focuses on reducing the overall number of possible ligands; in the later stages, during lead-optimization, the emphasis shifts to reducing experimental costs and the duration of time required to make a discovery. Applied ligand-based virtual screening using Volsurf and Molegro descriptors and a random forest algorithm (a method of machine learning) were included in the structure-based virtual screening.

Once AD evidence an activation of inflammatory pathways (Wyss-Coray and Rogers, 2012) and caulerpin present considerable anti-inflammatory activity, in this study, we created a database of caulerpin analogs and evaluated it with a ligand-based model that included molecular descriptors, as well as with a structure-based approach that included docking studies of monoamine oxidase B (MAO-B) inhibitors.

Materials and methods

Database

From the ChEMBL database, we selected a diverse set of 1523 structures (https://www.ebi.ac.uk/chembl/), which had been screened (*in vitro*) to inhibit the single protein of human monoamine oxidase B (Supporting Information Table S1). The compounds were classified using values of -logIC_{50} (mol/l) = pIC_{50}, which led us to assign 696 actives ($IC_{50} \geq 6$) and 827 in-actives ($IC_{50} < 6$). In this case, IC_{50} represented the concentration required for 50% inhibition of the single protein of human MAO-B. The database that included caulerpin (CLP001) and its 108 analogs (CLP002-109) was selected to build in our database. For all structures, SMILES codes were used as input data in a Marvin 14.9.1.0, 2014, ChemAxon (http://www.chemaxon.com). We used Standardizer software [JChem 14.9.1.0, 2014; ChemAxon (http://www.chemaxon.com)] to canonize structures, add hydrogens, perform aromatic form conversions, clean the molecular graph in three dimensions, and save compounds in sdf format (Imre et al., 2003).

Volsurf descriptors

Three-dimensional structures (3D) were used as input data in the Volsurf+ program v. 1.0.7 (Cruciani et al., 2000) and were subjected to molecular interaction fields (MIF) (Cruciani et al., 2000) to generate descriptors using the following probes: N1 (amide nitrogen-hydrogen bond donor probe), O (carbonyl oxygen-hydrogen bond acceptor probe), OH2 (water probe), and DRY (hydrophobic probe). Additional non-MIF-derived descriptors were generated to create a total of 128 descriptors (Cruciani et al., 2000). Volsurf descriptors have been previously used to predict the inhibitory actions of flavonoids against enzymes (Scotti et al., 2011).

Drug-like score

Structures were used as input data in DRAGON Professional version 6.0.30 to generate Dragon drug-like consensus, which was calculated as a mean of 7 drug-like scores that were based on the following: Lipinski's rules (Lipinski et al., 2001); the drug-like filter produced by Oprea et al. (2000); the drug-like score implemented by Walters (Walters and Murcko, 2002); the drug-like filter produced by Chen (Chen et al., 2005); the drug-like score that was based on two rules proposed by Zheng (Zheng et al., 2005); the drug-like score that was proposed by Rishton (Rishton, 2003); and the drug-like filter implemented by Veber and co-workers (Veber et al., 2002).

Models

Knime 2.10.0 software (KNIME 2.10.0 the Konstanz Information Miner Copyright, 2003–2014, www.knime.org) (Berthold et al., 2007) was used to perform all of the following analyses. The descriptors and class variables were imported from the Volsurf+ program, v. 1.0.7, and the data were divided using the "Partitioning" node with the "stratified sample" option to create a training set and a test set, encompassing 80% and 20% of the compounds, respectively. Although the compounds were selected randomly, the same proportion of active and inactive samples was maintained in both sets. For internal validation, we employed cross-validation using ten randomly selected, stratified groups, and the distributions according to activity class variables was found to be maintained in all validation groups and in the training set. Descriptors were selected, and a model was generated using the training set and the Random Forest algorithm (RF) (Breiman, 2001), using the WEKA nodes (Hall et al., 2009). The parameters selected for RF included the

Table 1
Summary of training, internal cross-validation, test results, and corresponding match results, which were obtained using the RF algorithm on the total set of 1523 compounds (1218 were in the training set and 305 in the test set).

	Training			Validation		Test		
	Samples	Match	%Match	Match	%Match	Samples	Match	%Match
Active	557	556	99.8	393	70.6	139	115	82.7
Inactive	661	659	99.7	662	74.5	166	142	85.5
Overall	1218	1215	99.8	886	72.7	305	257	84.3

following settings: number of trees to build = 50, seed for random number generator = 1, for training and internal cross-validation sets. The internal and external performances of the selected models were analyzed for sensitivity (true positive rate, *i.e.*, active rate), specificity (true negative rate, *i.e.*, inactive rate), and accuracy (overall predictability). Additionally, the sensitivity and specificity of the Receiver Operating Characteristic (ROC) curve was find to describe true performance with more clarity than accuracy. The plotted ROC curve shows the true positive (active) rate either versus the false positive rates, *i.e.* sensitivity versus (1-specificity). In a two-class classification, when a variable that is being investigated cannot be distinguished between the two groups (*i.e.*, when there is no difference between the two distributions), the area under the ROC curve equals 0.5, which is to say that the ROC curve will coincide with the diagonal. When there is a perfect separation of values between two groups (*i.e.*, no overlapping of distributions), the area under the ROC curve equals 1, which is to say that the ROC curve will reach the upper left corner of the plot (Hanley and McNeil, 1982). Additionally, we calculated the Mathews correlation coefficient, wherein a value of 1 represents a perfect prediction, a value of 0 represents a random prediction, and a value of −1 represents total disagreement between prediction and observation.

Docking

The structure of MAO-B in complex with rosiglitazone (PDB ID 4A7A) (Binda et al., 2012) was downloaded from the Protein Data Bank (http://www.rcsb.org/pdb/home/home.do). Alkaloid structures were submitted to molecular docking using the Molegro Virtual Docker, v. 6.0.1 (MVD) (Thomsen and Christensen, 2006). All of the water compounds were deleted from the enzyme structure, and the enzyme and compound structures were prepared using the same default parameter settings in the same software package (Score function: MolDock Score; Ligand evaluation: Internal ES, Internal HBond, Sp2–Sp2 Torsions, all checked; Number of runs: 10 runs; Algorithm: MolDock SE; Maximum Interactions: 1500; Max. population size: 50; Max. steps: 300; Neighbor distance factor: 1.00; Max. number of poses returned: 5). The docking procedure was performed using a GRID of 15 Å in radius and 0.30 in resolution to cover the ligand-biding site of the MAO-B structure. Templates with features expected to be relevant for ligand binding (rosiglitazone) were generated to perform docking. The Moldock score [GRID] algorithm was used as the score function, and the Moldock search algorithm was used (Thomsen and Christensen, 2006).

Results and discussion

The Volsurf (v 1.0.7) program generated 128 descriptors that, together with the dependent variables (binary classification) that described whether the compounds were active (A) or inactive (I), were used as input data in the Knime program (v. 2.10.0) to generate the Random Forest model. For all 1523 compounds that comprised the training data sets, the generation of all 128 descriptors by Volsurf+ took approximately 20 min using a computer with an i7 processor, running at 3.4 GHz, and equipped with 12 GB of RAM memory.

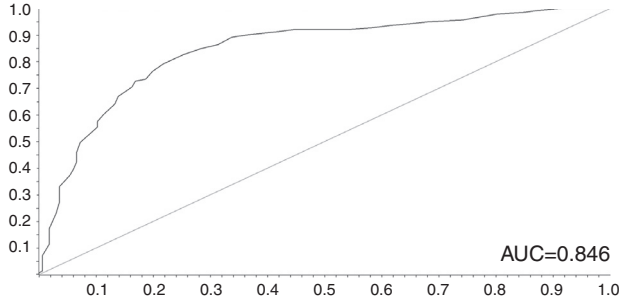

Fig. 1. Receiver Operating Characteristic (ROC) plot, sensitivity versus 1-specificity, generated by the selected Random Forest model for test set and value of the area under the curve (AUC).

Table 1 summarizes the statistical indices of the RF model for the training, cross-validation, and test sets. For the training set, the learning machine program gave similar hit rates for the inactive compounds and active compounds, which were above 99.7%. However, for the cross-validation and test sets, the RF model was better at predicting the inactive compounds; therefore, the specificity (true negative rate) was higher for the cross-validation and test sets (74.5% and 85.5%, respectively) than the sensitivity (true positive rate), which was measured to be 70.6% and 82.7%, respectively (Table 1). Because the false positive rate (1-specificity) was significantly lower, there was only 25.5% and 14.5% specificity for the cross-validation and test sets (Table 1), respectively. Therefore, compounds selected by the model as active had a low probability of being false positives (*i.e.*, of being inactive). These results are illustrated in Table 1 as well as in the ROC (Receiver Operating Characteristic) plot that was generated for the test set, which plotted the true positive (active) rate against the false positive rates and had an area under the curve value of approximately 0.846 (Fig. 1), which is close to 1.

The Matthews Correlation Coefficient (MCC) values for the training, cross-validation and test sets were 0.99, 0.46 and 0.68, respectively. Because an MCC value of 1 represents a perfect prediction, a value of 0 represents a random prediction, and a value of −1 indicates total disagreement between prediction and observation, the RF model indicated that the values of MCC that were calculated were significant, particularly with respect to the training and test sets. The equation used to obtain these values is as follows:

$$\mathrm{MCC} = \frac{\mathrm{TP} \times \mathrm{TN} - \mathrm{FP} \times \mathrm{FN}}{\sqrt{(\mathrm{TP}+\mathrm{FP})(\mathrm{TP}+\mathrm{FN})(\mathrm{TN}+\mathrm{FP})(\mathrm{TN}+\mathrm{FN})}},$$

where TP = true positive rate, TN = true negative rate, FP = false positive rate, and FN = False negative rate.

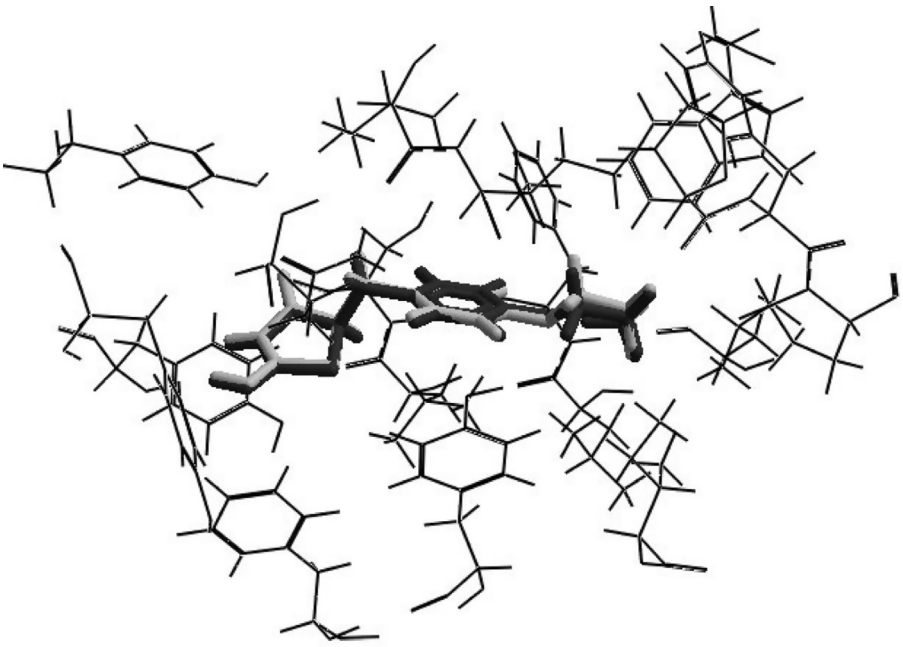

Fig. 2. Superposition of crystal pose (black) and docking pose (gray) validating the methodology.

Docking was validated redocking the original ligand rosiglitazone in active site of MAO-B as observed in crystallography pdb file (PDB ID 4A7A) (Binda et al., 2012). The same parameter describes to evaluate caulerpin and analogs was used in validation. Superposition of poses is represented in Fig. 2 and shows a perfect match.

Initially, we sought to evaluate the potential of using caulerpin as an MAO-B inhibitor. The results presented in Table 2 indicate that caulerpin exhibits potential inhibitory activity and can therefore be used as a lead. As we aimed to include a restrictive screening in this study, we selected 33 as the perceptual limit for our docking methodology, such that only the analogs that had energy lower than a −151.87 Moldock score (*i.e.*, the lowest 33% of MolDock energies of the whole database) were selected as active. The Volsurf program (v. 1.0.7) generated 128 descriptors that, together with a dependent variable (binary classification), described whether a compound was active (A) or inactive (I); these were used as input data in the Knime software program (v. 2.10.0). From the RF model, we selected the compounds classified as being active (*i.e.*, having a predicted probability of greater than 50%). Crossing the results, we observed a consensus of 56.9% between the methodologies. Using the mixed ligand-based and structure-based approach, we selected nine active analogs of caulerpin (**21**).

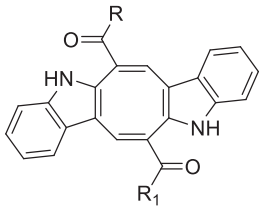

21

In analyzing the five best analogs from each methodological approach, we observed a clear connection between the values obtained for the compounds CLP 012, CLP 068, CLP 078 and CLP 100, which were the lead results in the two studies. In evaluating the chemical characteristics from the active analogs, we observed that a monosubstitution that was symmetrical with chlorine and methyl at positions 4 and 4′ and 5 and 5′, respectively, was not significantly changed compared to caulerpin (**21**). However, the presence of an amide or acyl halide polar group in R and a short nonpolar allyl or butyl chain in R1 generated lower docking energies and higher predicted probability. All active analogs exhibited favorable values in the dragon consensus of their drug-like scores (the consensus is calculated as the mean of the results of seven drug-like scores). With the exception of CLP109, all active analogs presented scores above 0.75 (Table 2), highlighting the promising scores of the leading analogs (CLP 012, CLP 068, CLP 078 and CLP 100), which had scores above 0.80. A drug-like score is a value ranging from 0 to 1, in which a value of 1 indicates that a compound is a potential drug candidate.

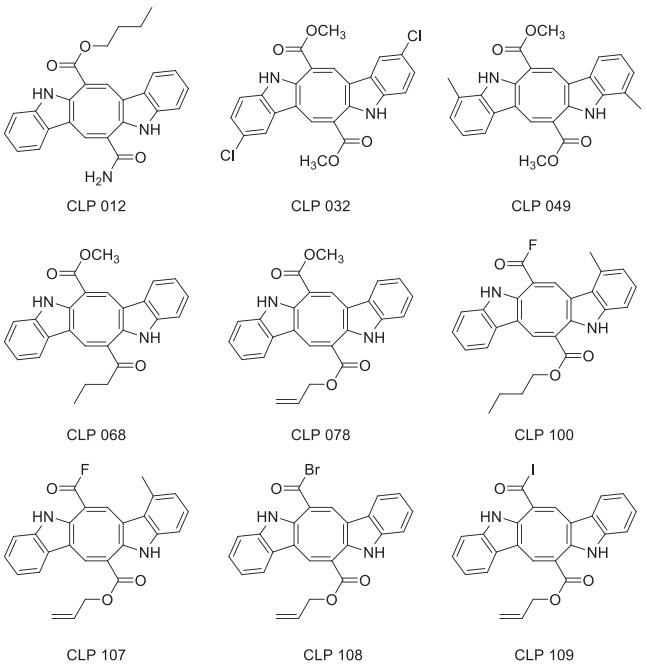

Table 2
Summary of the Moldock energy, predicted probability (%) and Dragon drug-like consensus of both caulerpin (CLP001) and of its analogs that were found to be active against MAO-B.

	Moldock energy	Predicted probability	Drug-like score
CLP001	−152	58	0.77
CLP012	−164	60	0.87
CLP032	−153	64	0.75
CLP049	−155	52	0.87
CLP068	−159	66	0.87
CLP078	−155	62	0.80
CLP100	−161	64	0.87
CLP107	−152	58	0.77
CLP108	−155	58	0.75
CLP109	−153	54	0.65

In corroborating the analysis of active compounds, several similar characteristics to the inactive group were observed, including the presence of groups with similar polarities in R or R1 (**21**). Whether in a symmetric (CLP 006 and CLP 009) or asymmetric (CLP 0013) context, the presence of a polar group was found to negatively influence performance. The same effect occurs in the presence of nonpolar groups (CLP 037 and CLP 074). The substitution of both indole nitrogens with alternative heteroatoms such as oxygen to serve as the binding groups of that position reduced the inhibitor effect (CLP 065 and CLP 022).

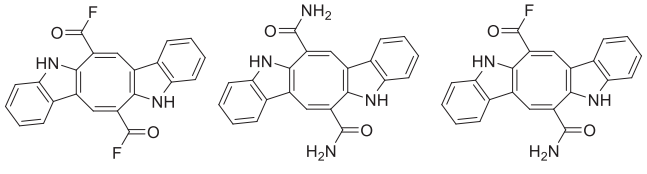
CLP 006

CLP 009

CLP 013

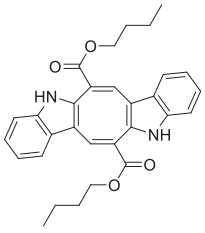
CLP 037

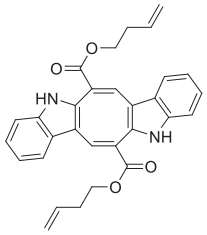
CLP 074

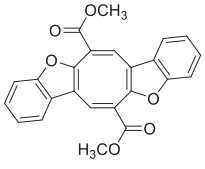
CLP 065

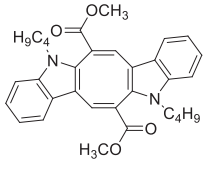
CLP 022

Although aromatic substitutions did not lead CLP 032 and CLP 049 to become more effective, both a change in position and disubstitution were found to significantly reduce potency (CLP 029, CLP 051, CLP 033 and CLP 057). Strong activators such as hydroxyl also decreased inhibitor activity (CLP 034 and CLP 036).

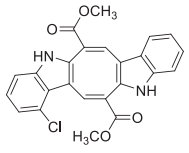
CLP 029

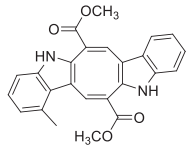
CLP 050

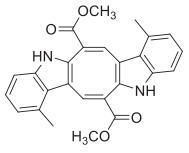
CLP 051

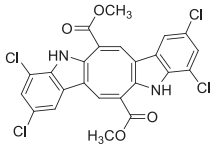
CLP 033

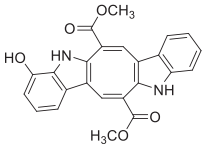
CLP 034

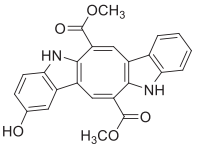
CLP 036

In Fig. 3, it is possible to observe the hydrogen bonding (H-bond) interactions between rosiglitazone (**A**), the drug utilized as template, and two caulerpin analogs, which were classified as active (CLP 012) (**B**) and inactive (CLP 006) (**C**). It is also possible to observe the interactions between the Tyr 435 (**A**) residue from MAO-B and rosiglitazone (**A**), and between Tyr 435(A) and CLP 012 (**B**). In CLP 012 (**D**) and CLP 006 (**E**), the electrostatic distribution is shown, corroborating the importance of polar (blue) and non-polar (green) substitutions to activity.

In this work, we identified the fundamental physical and chemical characteristics of caulerpin analogs (**21**) and indicated a possibility of how they can produce inhibitory effects against MAO-B. Ligand and structure-based results, associated with drug-like score, allow us to indicate the potential possibility of using this skeleton as a tool against AD in future studies.

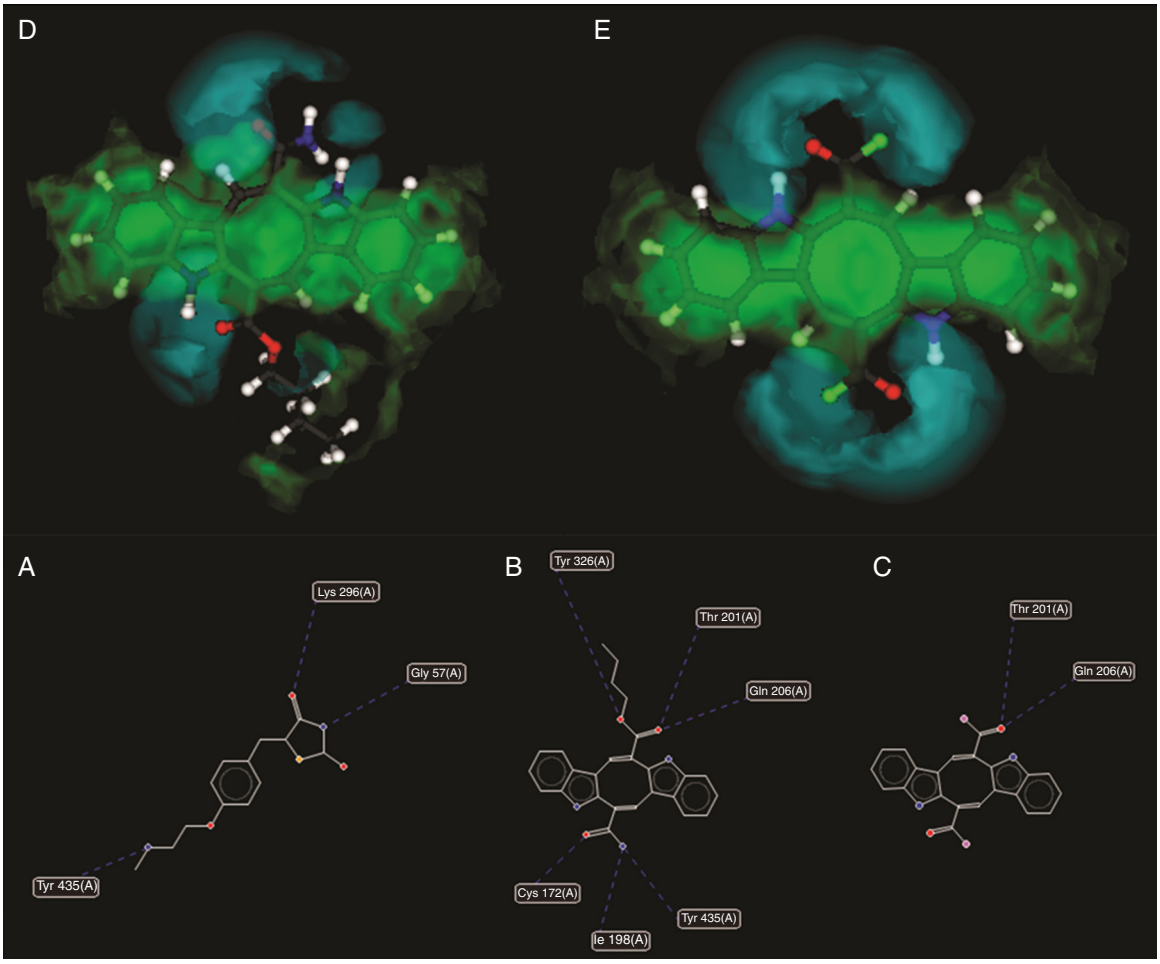

Fig. 3. Hydrogen bonding interactions of rosiglitazone (A), CLP 012 (B) and CLP 006 (C) with MAO-B and their electrostatic distributions on CLP 012 (D) and CLP 006 (E).

Conflicts of interest

The authors declare no conflicts of interest.

Authors' contributions

VPL produced the analogs and performed the docking study. MTS and LS created the ligand based model. All of the authors have read the final manuscript and have agreed to its submission for appraisal.

Acknowledgment

The authors would like to thank the Brazilian National Counsel of Technological and Scientific Development (CNPq) for financial support.

Appendix A. Supplementary data

Supplementary data associated with this article can be found, in the online version, at doi:10.1016/j.bjp.2015.08.005.

References

Baunbaek, D., Trinkler, N., Ferandin, Y., Lozach, O., Ploypradith, P., Rucirawat, S., Ishibashi, F., Iwao, M., Meijer, L., 2008. Anticancer alkaloid lamerallins inhibit protein kinase. Mar. Drugs 6, 514–527.

Berthold, M.R., Cebron, N., Dill, F., Gabriel, T.R., Kötter, T., Meinl, T., Ohl, P., Sieb, C., Thield, K., Wiswedel, B., 2007. In: Preisach, C., Burkhrdt, H., Schimidt-Thieme, L., Decker, R. (Eds.), Data analysis, machine learning and applications. Springer, Berlin, pp. 319–326.

Bidon-Chanal, A., Fuertes, A., Alondo, D., Perez, D.I., Martinez, A., Luque, F.J., Medina, M., 2013. Evidence for a new binding mode to GSH-3β: allosteric regulation by the marine compound palinurin. Eur. J. Med. Chem. 60, 479–489.

Binda, C., Aldeco, M., Geldenhuys, W.J., Tortorici, M., Mattevi, A., Edmondson, D.E., 2012. Molecular insights into human Monoamine Oxidase B inhibition by the glitazone anti-diabetes drugs. Med. Chem. Lett. 3, 39–42.

Binda, C., Milczek, E.M., Bonivento, D., Wang, J., Mattevi, A., Edmondson, D.E., 2011. Lights and shadows on monoamine oxidase inhibition in neuroprotective pharmacological therapies. Curr. Top. Med. Chem. 11, 2788–2796.

Bolea, I., Gella, A., Unzeta, M., 2013. Propargylamine-derived multitarget-directed ligands: fighting Alzheimer's disease with monoamine oxidase inhibitors. J. Neural Transm. 120, 893–902.

Breiman, L., 2001. Random forests. Mach. Learn. 45, 5–32.

Cavalcante-Silva, L.H.A., Correia, A.C.C., Barbosa-Filho, J.M., Silva, B.A., Santos, B.V.O., Lira, D.P., Miranda, G.E.C., Cavalcante, F.A., Moreira, M.S.A., 2013. Spasmolytic effect of caulerpin involves blockade of Ca influx on guinea pig ileum. Mar. Drugs 11, 1553–1564.

Chen, G., Zheng, S., Luo, X., Shen, J., Zhu, W., Liu, H., Gui, C., Zhang, J., Zheng, M., Puah, C.M., Chen, K., Jiang, H., 2005. Focused combinatorial library design based on structural diversity, druglikeness and binding affinity score. J. Comb. Chem. 7, 398–406.

Choi, B.W., Ryu, G., Park, S.H., Kim, E.S., Shin, J., Roh, S.S., Shin, H.C., Lee, B.H., 2007. Anticholinesterase activity of plastoquinones from *Sargassum sagamianum*: lead compounds for Alzheimer's diseases therapy. Phytother. Res. 21, 423–426.

Choi, D.Y., Choi, H., 2015. Natural products from marine organisms with neuroprotective activity in the experimental models of Alzheimer's disease, Parkinson's disease and ischemic brain stroke: their molecular targets and action mechanisms. Arch. Pharm. Res. 38, 139–170.

Cruciani, G., Crivori, P., Carrupt, P.A., Testa, B., 2000. Molecular fields in quantitative structure-permeation relationships: the Volsurf approach. J. Mol. Struc. Theochem. 503, 17–30.

Custódio, L., Justo, T., Silvestre, L., Barradas, A., Duarte, C.V., Pereira, H., Barreira, L., Rauter, A.P., Alberío, F., Varela, J., 2012. Microalgae of different phyla display antioxidant, metal chelating and acetylcholinesterase inhibitors activities. Food Chem. 131, 134–140.

Debdab, M., Renault, S., Lozach, O., Meijer, L., Paquin, L., Carreaux, F., Bazureau, J.P., 2010. Synthesis and preliminary biological evaluation of new derivatives of the marine alkaloid leucettamine B as kinase inhibitors. Eur. J. Med. Chem. 45, 805–810.

Fernandez, H.H., Chen, J.J., 2007. Monoamine oxidase-B inhibition in the treatment of Parkinson's disease. Pharmacotherapy 27, 174–185.

Gerwick, W.H., Moore, B.S., 2012. Lessons from the past and charting the future of marine natural products drug discovery and chemical biology. Chem. Biol. 19, 85–98.

Gul, W., Hamann, M.T., 2005. Indole alkaloid marine natural products: an established source of cancer drugs leads with considerable promise for the control of parasitic, neurological and other diseases. Life Sci. 78, 442–453.

Hall, M., FranK, E., Holmes, G., Pfahringer, B., Reutemann, P., Witten, I.H., 2009. The WEKA data mining software: an update. SIGKDD Exploration 11.

Hamann, M., Alonso, D., Martin-Aparicio, E., Fuertes, A., Pérez-Puerto, M.J., Castro, A., Morales, S., Navarro, M.L., Del Monte-Millán, M., Medina, M., Pennaka, H., Balaiah, A., Peng, J., Cook, J., Wahyuono, S., Martínez, A., 2007. Glycogen synthase kinase (GSK-3β) inhibitory activity and structure activity relationship (SAR) studies of themanzamine alkaloids. Potencial for Alzheimer's disease. J. Nat. Prod. 70, 1397–1405.

Hanley, J.A., McNeil, B.J., 1982. The meaning and use of the area under a receiver operation characteristic (ROC) curve. Radiology 143, 29–36.

Imre, G., Veressc, G., Volfordd, A., Farkas, Ö., 2003. Molecules from the Minkowski space: an approach to building 3D molecular structure. J. Mol. Struc. Theochem. 666, 51–59.

Jin, D.Q., Lim, C.S., Sung, J.Y., Choi, H.G., Ha, I., Han, J.S., 2006. Ulva conglabata, a marine algae, has neuroprotective and anti-inflammatory effects in murine hippocampal and microglial cells. Neurosci. Lett. 402, 154–158.

LaFerla, F.M., Oddo, S., 2005. Alzheimer's disease: abeta, tau and synaptic dysfunction. Trends Mol. Med. 11, 170–176.

Langjae, R., Bussarawit, S., Yuenyongsawad, S., Ingkaninan, K., Plubrukarn, 2007. Acetylcholinesterase-inhibiting steroidal alkaloid from the sponge *Corticium* sp. Steroids 72, 682–685.

Lill, M.A., Danielson, M.L., 2011. Computer-aided drug design platform using PyMOL. J. Comput. Aided Mol. Des. 25, 13–19.

Lipinski, C.A., Lombardo, F., Dominy, B.W., Feeney, P.J., 2001. Experimental and computational approaches to estimate solubility and permeability in drug discovery and development settings. Adv. Drug. Deliver. Rev. 46, 3–26.

Liu, C.-C., Kanekiyo, T., Xu, H., Bu, G., 2013. Apolipoprotein E and Alzheimer disease: risk, mechanisms and therapy. Nat. Rev. Neurol. 9, 106–118.

Mayer, A.M.S., Rodrígiez, A.D., Berlink, R.G.S., Fusetani, N., 2011. Marine pharmacology in 2007-8: marine compounds with antibacterial, anticoagulant, antifungal, anti-inflammatory, antimalarial, antiprotozoal, antituberculosis, and antiviral activities; affecting the immune and nervous system, and other miscellaneous mechanism of action. Comp. Biochem. Physiol. 153, 191–222.

Meijer, L., Thunnissen, A.M.W.H., White, A.W., Garnier, M., Nokolic, M., Tsai, L.H., Walter, J., Cleverley, K.E., Salinas, P.C., Wu, Y.-Z., Bienart, J., Mandelkow, E-M., Kim, S.H., Petit, G.R., 2000. Inhibition of cyclin-dependet kinase, GSK-3β and CSK1 by hymenialdisine, a marine sponge constituent. Chem. Biol. 7, 51–63.

Meijer, L., Skaltsounis, A.L., Magiatis, P., Polychronopoulus, P., Knockaert, M., Leost, M., Ryan, X.P., Vonica, C.A., Brivanlou, A., Dajani, R., Crovace, C., Tarricone, C., Musacchio, A., Roe, S.M., Pearl, L., Greengard, P., 2003. GSK-3-selective inhibitors derived from tyrian purple indirubins. Chem. Biol. 10, 1255–1266.

Motohashi, K., Toda, T., Sue, M., Furihata, K., Shizuri, Y., Matsuo, Y., Kasai, H., Shinya, K., Takagi, M., Izimikawa, M., Horikawa, Y., Seto, H., 2010. Isolation and structure elucidation of tumescenamides A and B, two peptides produced by *Streptomyces tumescens* YM23-260. J. Antibiot. 63, 549–552.

Oprea, T.I., Sherbukhin, V., Svensson, P., Kuhler, T.C., 2000. Chemical information management in drug discovery: optimizing the computational and combinatorial chemistry interfaces. J. Mol. Graph. Model. 18, 512–524.

Patil, P.O., Bari, S.B., Firke, S.D., Deshmukh, P.K., Donda, S.T., Patil, D.A., 2013. A comprehensive review on synthesis and designing aspects of coumarin derivatives as monoamine oxidase inhibitors for depression and Alzheimer's disease. Bioorg. Med. Chem. 21, 2434–2450.

Radwan, M.A., El-Sherbiny, M., 2007. Synthesis and antitumor activity of indolylpyrimidines: marine natural product meridianin D analogues. Bioorg. Med. Chem. 15, 1206–1211.

Riediger, N.D., Othman, R.A., Suh, M., Moghadasian, M.H., 2009. A systemic review of the roles of n-3 fatty acid in health and diseases. J. Am. Diet. Assoc. 109, 669–679.

Rishton, G.M., 2003. Nonleadlikeness and leadlikeness in biochemical screening. Drug Discovery Today 8, 86–96.

Schumacher, M., Kelkel, M., Dicato, M., Diederich, M., 2011. Gold from the sea: marine compounds inhibitors of the hallmarks of cancer. Biotechnol. Adv. 29, 531–547.

Scotti, L., Fernandez, M.B., Muramatsu, E., Pasqualoto, K.F.M., Emereciano, V.D., Tavares, L.C., Silva, M.S., Scotti, M.T., 2011. Self-organizing maps and Volsurf approach to predict aldose reductase inhibition by flavonoid compounds. Rev. Bras. Farmacog. 21, 170–180.

Souza, E.T., Queiroz, A.C., Miranda, G.E.C., Lorenzo, V.P., Silva, E.F., Freire-Dias, T.L.M., Cupertino-Silva, Y.K., Melo, G.M.A., Santos, B.V.O., Chaves, M.C.O., Alexandre-Moreira, M.S., 2009a. Antinociceptive activities of crude methanolic extract and phases, n-butanolic, chloroformic and ethyl acetate from *Caulerpa racemosa* (Caulerpaceae). Rev. Bras. Farmacog. 19, 115–120.

Souza, E.T., Pereira, D.L., Queiroz, A.C., Miranda, G.E.C., Lorenzo, V.P., Silva, D.J.C., Bezerra, A.A., Campessato, E.A.M., Araújo-Júnior, J.X., Barbosa-Filho, J.M., Athayde-Filho, P.F., Santos, B.V.O., Chaves, M.C.O., Alexandre-Moreira, M.S., 2009b. The antinociceptive and anti-inflammatory activities of Caulerpin, a bisindole alkaloid isolated from seaweeds of the genus *Caulerpa*. Mar. Drugs 7, 689–704.

Talete srl, Dragon (Software for Molecular Descriptor Calculation) Version 6.0. (2014). http://www.talete.mi.it/.

Thomas, N.V., Kim, S.-K., 2011. Potential pharmacological applications of polyphenolic derivatives from marine brown algae. Environ. Toxicol. Pharmacol. 32, 325–335.

Thomsen, R., Christensen, M.H., 2006. Moldock: a new technique for high-accuracy molecular docking. J. Med. Chem. 49, 3315–3321.

Tian, L.W., Feng, Y., Shimizu, Y., Pfeifer, T.A., Wellington, C., Hooper, J.N.A., Quinn, R.J., 2014. ApoE secretion modulating bromotyrosine derivate from the Australian marine sponge *Callyspongia* sp. Bioorg. Med. Chem. Lett. 24, 3537–3540.

Turk, T., Avgustin, J.A., Batista, U., Strugar, G., Kosmina, R., Civovic, S., Janussen, D., Kauferstein, S., Mebs, D., Sepcic, K., 2013. Biological activities of ethanolic extracts from deep sea Antarctic marine sponges. Mar. Drugs 11, 1126–1139.

Veber, D.F., Johnson, S.R., Cheng, H.Y., Smith, B.R., Ward, K.W., Kopple, K.D., 2002. Molecular properties that influence the oral bioavailability of drug candidates. J. Med. Chem. 12, 2615–2623.

Walters, W.P., Murcko, M.A., 2002. Prediction of 'drug-likeness'. Adv. Drug Deliv. Rev. 54, 255–271.

Wyss-Coray, T., Rogers, J., 2012. Inflammation in Alzheimer disease – a brief review of the basic science and clinical literature. Cold Spring Harb. Perspect. Med. 2, a006346.

Yang, C.G., Liu, G., Jiang, B., 2002. Preparing functional bis (indole) pyrazine by stepwise cross-coupling reactions: an efficient method to construct the skeleton of dragmacidin D. J. Org. Chem. 67, 9392–9396.

Yoon, N.Y., Lee, S.H., Li, Y., Kim, S.K., 2009. Phlorotannins from *Ishige okamurae* and their acetyl and butylcholinesterase inhibitors effects. J. Func. Foods 1, 331–335.

Zheng, S., Luo, X., Chen, G., Zhu, W., Shen, J., Chen, K., Jiang, H., 2005. A new rapid and effective chemistry space filter in recognizing a druglike database. J. Chem. Inf. Model. 45, 856–862.

Zhu, W., Xie, W., Pan, T., Jankovic, J., Li, J., Youdim, M.B., Le, W., 2008. Comparison of neuroprotective and neurorestorative capabilities of rasagiline and selegiline against lactacystin-induced nigrostriatal dopaminergic degeneration. J. Neurochem. 105, 1970–1978.